Preparation of Dynamically Vulcanized Thermoplastic Elastomer Nanocomposites Based on LLDPE/Reclaimed Rubber

Fatemeh Razmjooei,[1] Ghasem Naderi,[2] Gholamreza Bakhshandeh[2]

[1]*Department of Polymer Engineering, Faculty of Graduate studies, Tehran South Branch, Azad University, Tehran, Iran*
[2]*Iran Polymer and Petrochemical Institute, Tehran, Iran*

Received 3 January 2011; accepted 31 August 2011
DOI 10.1002/app.35558
Published online 7 December 2011 in Wiley Online Library (wileyonlinelibrary.com).

ABSTRACT: Dynamically vulcanized thermoplastic elastomers nanocomposites (TPV nanocomposites) based on linear low density polyethylene (LLDPE)/reclaimed rubber/organoclay were prepared via one-step melt blending process. Maleic anhydride grafted polyethylene (PE-*g*-MA) was used as a compatibilizing agent. The effects of reclaimed rubber content (10, 30, and 50 wt %), nanoclay content (3, 5, and 7 wt %), and PE-*g*-MA on the microstructure, thermal behavior, mechanical properties, and rheological behavior of the nanocomposites were studied. The TPV nanocomposites were characterized by X-ray diffraction, transmission electron microscopy, scanning electron microscopy (SEM), differential scanning calorimeter, mechanical properties, and rheometry in small amplitude oscillatory shear. SEM photomicrographs of the etched samples showed that the elastomer particles were dispersed homogeneously throughout the polyethylene matrix and the size of rubber particles was reduced with introduction of the organoclay particles and compatibilizer. The effects of different nanoclay contents, different rubber contents, and compatibilizer on mechanical properties were investigated. Increasing the amount of nanoclay content and adding the compatibilizer result in an improvement of the tensile modulus of the TPV nanocomposite samples. © 2011 Wiley Periodicals, Inc. J Appl Polym Sci 124: 4864–4873, 2012

Key words: linear low density polyethylene; reclaimed rubber; nanocomposites; thermoplastic vulcanized; compatibilizer

INTRODUCTION

Thermoplastic elastomers (TPEs) are a new class of materials that behave like thermoset rubbers, but are processed and converted via thermoplastic techniques such as injection molding, extrusion, blow molding, and thermoforming. Thermoplastic vulcanized (TPVs) are a special type of thermoplastic elastomers, which are produced via crosslinking of the rubber phase during melt mixing of the rubber and thermoplastic phase. TPVs exhibit intermediate cost, good chemical resistance, good dynamic properties, high weatherability (measured characteristic that shows how well a product performs during exposure to outdoor weather conditions), and low compression set in comparison with simple blends of thermoplastic elastomers.[1] Many commercial TPVs have been developed for various applications in seals, wire and cable, food closures, bumpers, automotive interiors, and medical industries because of their excellent weatherability, low density, and relatively low manufacturing cost.[2] The TPV blends are often reinforced by stiff fillers such as glass fiber, carbon black, talc, and calcium carbonate at a high-loading level to improve mechanical properties. These fillers also increase the weight of the TPV blends, rending them less attractive for automotive and aerospace applications.[2–4]

One of the various problems that mankind faces as it enters into the 21st century is the problem of disposal management of waste rubbers with development of rubber industry.[5,6] Recycle of the scrap rubber in the form of reclaimed rubber is one of the most desirable approaches to solve the disposal problem. A more direct environmental and economical benefit of rubber recovery is the replacement of the rubber phase of some TPVs with reclaimed rubber.

The major criteria for the formation of thermoplastic elastomers is that the two components of thermoplastic elastomer must be thermodynamically incompatible enough to phase separate, but not so dissimilar that intimate intermixing can not be accomplished. To achieve this condition, one or some compatibilizer agents should be introduced into the system. Also, compatibilizer can be premade

Correspondence to: G. Naderi (g.naderi@ippi.ac.ir or Ghasem.naderi@polymtl.ca).

and added to the immiscible polymer blends, and the latter procedure is called reactive compatibilization.[7]

Several studies have been conducted on the development of polyethylene/rubber (PE/rubber) blends such as PE/natural rubber (PE/NR), PE/ground tire rubber (PE/GTR), and PE/reclaimed rubber. Ahmad et al.[8] have examined the effects of different fillers on the mechanical properties of NR/linear low density polyethylene (NR/LLDPE) blends. The studies showed that the polymer–filler interactions and mean agglomerate particle size of dispersed phase have a significant influence on the mechanical properties of samples.[8] Magaraphan et al.[9] have studied the effects of the maleic anhydride (MA) as a compatibilizer on the morphology of LLDPE/NR blends and showed that the *in situ* copolymer is capable of promoting good interfacial adhesion, consequently enhanced mechanical properties. Moreover, the copolymer containing fine fibrils and more links between domains plays a key role in inducing compatible blends.[9] Abadchi et al.[10] have studied the effect of partial replacement of NR by GTR on the morphology, rheology, and mechanical properties of LLDPE/NR/GTR terpolymer composition. The latter study showed that using MA and dicumyl peroxide during melt mixing, concluded to a better dispersion of GTR, formation of a morphology similar to that of a dynamic vulcanized thermoplastic elastomers, and also an improvement in the interfacial bonding between phases and dramatically increase in the mechanical properties.[10] Punnarak et al.[11] have considered the effects of different curing systems on the mechanical properties of high density polyethylene/reclaimed rubber (HDPE/RR) and found a better improvement in the mechanical properties of the blend using sulphur curing system rather than other curing systems.[11] Kumar et al.[12] have studied the effects of different cure systems namely sulphuric, phenolic, and peroxide curing systems and also different fresh rubbers namely ethylene propylene diene monomer (EPDM), styrene–butadiene–rubber (SBR), and NR on the mechanical properties of the LDPE/fresh rubber/GTR blend. The studies showed that sulphuric and phenolic-curing agents are most suitable for dynamic curing. Additionally, the thermoplastic dynamic vulcanizates with the best mechanical performance contained SBR and EPDM rubbers. The observed improvements in mechanical performance were attributed to the chain entanglement and co-crosslinking in the interphase between the devulcanized ground tire rubber particles and the surrounding matrix.[12] Scaffaro et al.[13] have studied the possibility to produce secondary materials by blending recycled polyethylene and GTR. The results indicated that the blends showed fairly good mechanical and rheological properties provided that relatively low concentrations of GTR and proper thermal conditions are adopted.[13]

The researches in polymer materials are increasingly focusing on the development of polymer nanocomposites, which have attracted considerable attention during the last decade. The mechanical properties of the composites filled with nanoparticles are generally superior to those filled with micron-sized particles of the same filler, owing to its extremely high aspect ratio and also due to the nanometer filler thickness comparable to the scale of the polymer chain structure.[14,15] Also, nanoparticles bring stronger interfacial interactions between the dispersed solids and the polymer matrix.[2]

Nanocomposites have been observed to exhibit dramatic increase in the physical properties such as barrier, flammability, thermal stability, and ablation performance depending on the dispersability of the organoclay in the matrix and extent of intercalation of the polymeric chains. Because of the nonpolar nature of LLDPE and the large surface area of polar nanoclay particles, it is challenging to achieve good dispersion of nanoclay in the LLDPE matrix.

Nanocomposites based on LLDPE,[16–21] and nanocomposites based on NR,[22–24] have been studied during the recent years. However, to the best of our knowledge, no studies regarding TPV nanocomposites prepared using LLDPE/reclaimed rubber and nanoclay have yet been published. In this article, we studied the effects of reclaimed rubber content, nanoclay content, and presence of compatibilizer on the microstructure, mechanical, and thermal behavior of resulting LLDPE/reclaimed rubber TPVs. For that purpose, we prepared several nanocomposites with LLDPE thermoplastic, reclaimed rubber, and Cloisite 20A using a melt-mixing process.

EXPERIMENTAL

Materials

The basic specifications of the reclaimed rubber, LLDPE, compatabilizer, and nanoclay employed in this study are reported in Table I. The reclaimed rubber was supplied by Isatiss Co. (a subsidiary of Yazd Tire Co., Iran). LLDPE (LL 0220 AA) was a general purpose film grade of PE, provided by Arak Petrochimical Co., Iran. MA-modified polyethylene (PE-*g*-MA, 1 wt % MA grafted) with sample code Karabond® EM2L was obtained by Karangin Manufactring Co., Iran. The nanoclay used was Cloisite® 20A, which is a natural montmorillonite modified with dimethyl dihydrogenated tallow ammonium ions provided by Southern Clay Products. Commercial curing agents and additives including Sulfur (S), stearic acid, zinc oxide (ZnO), 2-mercaptobenzothiazole (MBT), and tetramethyl

TABLE I
Materials Specification

Materials	Commercial name	Characteristics
Linear low density polyethylene (LLDPE)	LLDPE 0220 AA	Density (g/cc): 0.92 MFI (g/10 min): 2.5 Melting Point (°C): 130
Reclaimed rubber (RR)	–	Density (g/cc): 1.18 Mooney viscosity, ML (1 + 4) at 100°C: 39.8 Acetone extract (%): 17.5
MA-modified polyethylene (PE-*g*-MA)	Karabond® EM2L	1 wt % maleic anhydride grafted
	Formulization of reclaimed rubber	
39% NR, 20% SBR, and BR	Oil (%)	5
	Rubber (%)	59
	Carbon black (%)	25.4
	Ash (%)	10.6
Nanoclay	Cloisite 20A	Density (g/cc): 1.77 CEC, mequiv/100 g clay: 95 X-ray diffraction, *d*-spacing (Å): 24.2

thiuram disulfide (TMTD) were provided by Bayer Co. The antioxidant (Irganox® B225) was supplied by Ciba Co., USA.

Sample Preparation

The TPV nanocomposite samples based on LLDPE/RR/Cloisite 20A were prepared by one-step melt-blending process in a brabender internal mixer for 16 min at 170°C with a rotor speed of 80 rpm. LLDPE, Cloisite 20A, reclaimed rubber, and the cure additives were added to the compound during melt blending, respectively. At first, the mixture of LLDPE and PE-MA was charged into the mixing chamber and melted for 2 min before addition of cloisite 20A. After introucing the nanoclay, blending process was continued for a further 4 min and then reclaimed rubber, and, finally, the cure system was added into the mixing chamber. In all above processes, nearly 0.5 wt % antioxidant was added during mixing. The blend samples were then compression molded at 170°C and 150 kg cm^{-2} for 10 min to form sheets with 1 mm thickness to obtain suitable samples for different tests. The ratios of LLDPE/RR were 90/10, 70/30, and 50/50 and the nanoclay concentration was 3, 5, and 7 wt %. The ratio of PE-*g*-MA/nanoclay was kept constant at 3: 1. The blend compositions are listed in Table II. The vulcanizing system was based on 100 phr reclaimed rubber, 2.5 phr ZnO, 1 phr stearic acid, 0.5 phr TMTD, 0.4 phr MBT, and 0.75 phr S. For comparison purposes, unfilled and uncompatibilized TPVs were also compounded as refrence matrials. In all instances, nanoclay had been dried at 90°C for 24 h before processing.

Characterization

To evaluate the dispersion state of the nanoclay in the polymer matrix, X-ray diffraction (XRD) was performed at room temperature using an X-ray diffractomer (Philips X'Pert) in the low angle of 2θ. The X-ray beam was a Cu Kα radiation (λ = 1.540598 Å) using a 50 kV voltage generator and a 40 mA current. The basal spacing of silicates was estimated from the position of the plane peak in the XRD intensity profile using the Bragg's law, $d = \lambda/(2 \sin \theta_{max})$. The nanostructure of the clay was observed by a transmission electron microscopy (TEM, Philips CM-200) with an accelerator voltage of 200 kV. The surface of the samples first coated with gold and then a thin section of each specimen was prepared by using a cryo-microtome equipped with a diamond knife. To study the morphology of the TPV nanocomposite samples, the cryogenically fractuted structures of the samples were etched by hot xylene to remove LLDPE phase. Treated samples were then coated with gold to avoid charging and viewed with a scanning electron microscope (SEM), Philips XL30. Rheological measurements of

TABLE II
Samples Codes and Their Compositions (wt %)

Sample codes	LLDPE	Reclaim rubber	Compatibilizer	Nanoclay
90/10/0	90	10	–	–
90/10/3	90	10	9	3
90/10/5	90	10	15	5
90/10/7	90	10	21	7
70/30/0	70	30	–	–
70/30/3	70	30	9	3
70/30/5	70	30	15	5
70/30/7	70	30	21	7
50/50/0	50	50	–	–
50/50/3	50	50	9	3
50/50/5	50	50	15	5
50/50/7	50	50	21	7
50/50/3-N	50	50	–	3
50/50/5-N	50	50	–	5
50/50/7-N	50	50	–	7

nanocomposite samples were conducted in parallel plate geometry with a diameter of 25 mm under nitrogen atmosphere at 170°C and in the frequency range of 0.03–100 Hz. The stress–strain properties of the composites were determined in accordance with the test procedures set forth in ASTM D 638 at room temperature with crosshead speed of 50 mm/min using an Instron model 6025. Crystallization behavior was studied using a Netzsch-DSC 200F3, differential scanning calorimeter (DSC) under nitrogen atmosphere. Samples were heated from 25 to 150°C at a rate of 10°C/min and then were cooled from 150 to 25°C at the same rate after holding at 150°C for 5 min to erase any thermal history effects. Melting temperture (T_m, °C) and melting enthalpy (ΔH_m, J/g) were obtained from the second heating run. Shore D type durometer was used to measure the hardness of the compounds according to ASTM D-2240.

RESULTS AND DISCUSSION

X-ray diffraction patterns

The X-ray diffraction (XRD) test is the most common powerful tool to study the dispersion state of organoclay particles inside the polymeric matrix. The XRD patterns of the pure organoclay (Cloisite 20A) and TPV nanocomposites prepared with LLDPE and 10, 30, and 50 wt % RR containing 5 wt % organoclay are shown in Figure 1. The distinct diffraction peak is observed for the pure organoclay at $2\theta = 3.44°$ corresponding to the basal spacing (d_{001}) of 2.56 nm. The d_{001} peak of the organoclay is also clearly observed in the samples prepared with the 10, 30, and 50 wt % RR, which has been shifted to lower angles, indicating an increase in the *d*-spacing of organoclay from 2.56 to 3.95 nm ($2\theta = 2.23°$), 4.18 nm ($2\theta = 2.11°$), and 4.8 nm ($2\theta = 1.85°$), for 90/10/5, 70/30/5, and 50/50/5 samples, respectively. Increasing the basal spacing of organoclay in the nanocomposite samples when compared with pure Cloisite 20A can be attributed to the penetration of polymeric chains into the silicate layers and development of an intercalated structure. The *d*-spacing of various samples is reported in Table III.

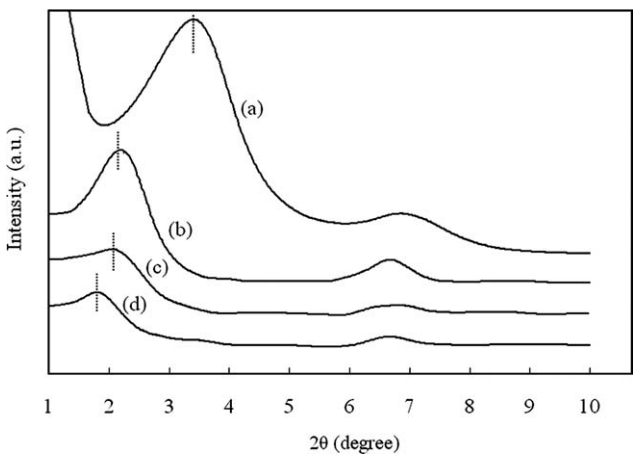

Figure 1 XRD patterns of (a) Cloisite 20A, (b) 90/10/5, (c) 70/30/5, and (d) 50/50/5.

TABLE III
Interlayer Spacing for Nanocomposite Samples

Sample codes (PE/reclaim/clay)	2θ (°)	*d*-Spacing (Å)
Cloisite 20A	3.44	$d_{001} = 25.6$
90/10/5	2.23	39.5
70/30/3	2.05	43.1
70/30/5	2.11	41.8
70/30/7	2.14	41.2
50/50/5	1.85	48
50/50/5-N	2.20	40

The interlayer distance of the organoclay in the nanocomposite samples increased as the elastomer contents increased. Therefore, higher nanoclay intercalation was achieved in the TPV nanocomposite prepared with 50 wt % of RR. The higher nanoclay intercalation means higher disordering of the layered silicate structure; consequently, the peak intensity of the clay in this sample was decreased.[25] In other words, the intensity of the XRD peaks in the TPV nanocomposites decreased, and the XRD peak shifted toward lower angles with an increase in the rubber contents as illustrated in Figure 1. The decrease in the intensity and the shift of XRD peak toward lower 2θ with increasing rubber contents indicate that the stacks of layered silicates have become yet more disordered or partially exfoliated. This means that the dynamic vulcanization of the rubber phase has increased the viscosity of the matrix, and hence the shear stress imposed by the matrix during the mixing is also increased, which in turn facilitates the break-up process of the nanoclay agglomerates and the incorporation of the polymer chains in the silicate galleries.[1] These results suggest that the clay disperses into both the LLDPE and the reclaimed rubber phases and that the clay concentration would increase in the rubber phase with increasing elastomer content. It has been reported that low torque in processing leads to poor clay dispersion in polymer nanocomposites.[26]

Figure 2 presents the torque traces for 90/10/5, 70/30/5, and 50/50/5 nanocomposite samples. These traces show that the torque enhanced with an increase in the RR concentration. This might be attributed to higher shear viscosity of the pure rubber than that of the pure LLDPE in the mixing conditions studied.

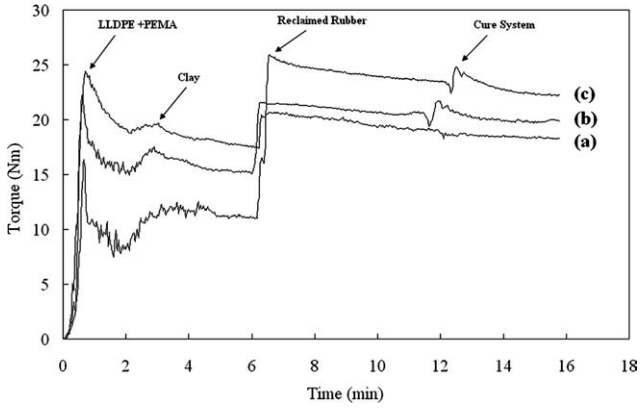

Figure 2 The mixing torque vs. time for (a) 90/10/5, (b) 70/30/5, and (c) 50/50/5

Figure 3 shows the XRD patterns of the original nanoclay and the samples containing 3, 5, and 7 wt % nanoclay contents in binary blends of 70/30 LLDPE/RR. The sample containing 3 wt % nanoclay shows a shift toward lower angles in the diffraction peak, which corresponds to a higher intergallery height in comparison with that of Cloisite 20A. Also, it can be seen that the diffraction peak of nanoclay was slightly shifted to higher angles with an increase in the nanoclay loading. In other words, the interlayer spacing of silicate galleries slightly decreases with clay loading. The lower *d*-spacing value is at filler loading 7 wt %. Also, the intensity of XRD peak of nanocomposites enhanced with increasing the clay content, because of the influence of the packing density, rending more difficult the penetration of the polymer chains between the silicate layers.[2]

Figure 4 presents the effect of compatibilizer on the XRD patterns of 50/50 LLDPE/RR blend containing 5 wt % organoclay. It can be seen that the interlayer distance of organoclay is larger in the sample with PE-*g*-MA than that of sample without

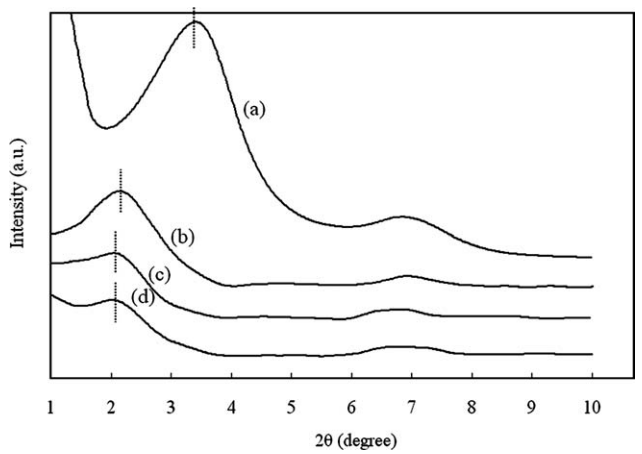

Figure 3 XRD patterns of (a) Cloisite 20A, (b) 70/30/7, (c) 70/30/5, and (d) 70/30/3

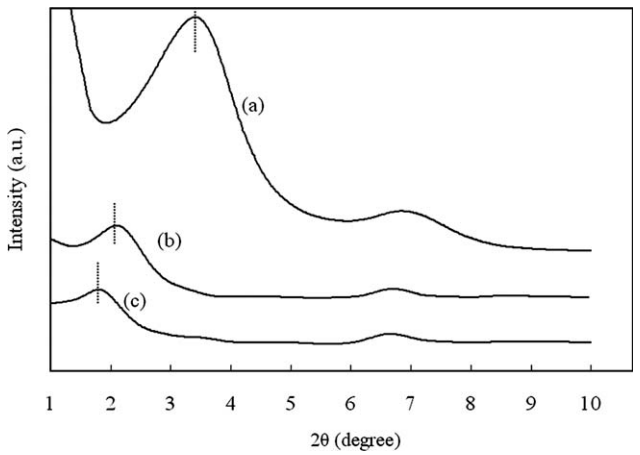

Figure 4 XRD patterns of (a) Cloisite 20A, (b) 50/50/5-N, and (c) 50/50/5

PE-*g*-MA ($2\theta = 2.2^\circ$, $d_{001} = 4$ nm). The shift in the diffraction peak toward lower angles may not always offer evidence for complete exfoliation, but may offer evidence for more disordered intercalation. This can be attributed to the penetration of polymeric and compatibilizer chains inside the silicate layers, which confirms the fact that polar functional groups of PE-*g*-MA cause more compatibility and development of interaction between nonpolar matrix with nanoclay and rubber phases to allow more intercalation. As it has been reported in the literature, it is very difficult for hydrophobic polymers such as LLDPE to intercalate into the organoclay layers, because LLDPE is so hydrophobic and lacks suitable interactions with the polar aluminosilicate surface of the nanoclay.[16,27,28] In general, surface compatibilization is required for low energy polymers such as polyolefines in order to reduce the large entropy difference between the polymer and the metallic clay surface to improve interface adhesion.[27] The MA-grafted LLDPE (PE-*g*-MA) has been used as a compatibilizer in this study, because it has good miscibility with nonpolar polymers and contains polar functional groups that can interact with the polar clays. When organoclay particles were later incorporated, their dispersion would be improved as a result of interaction between the MA carbonyl and the clay silanol group, promoting the carbonyl-silanol interface interaction with the formation of hydrogen bonds.[27] In general, MA is used as a reactive reagent to enhance the compatibilization of LLDPE and rubber phase.[9] This would reduce the energy barrier and therefore enhance interphase miscibility. As it has been shown in Figure 4(b), the d_{001} peak of the organoclay in the sample prepared with the 50 wt % rubber without compatibilizer has been shifted to low angles, which implies an increase in the *d*-spacing of organoclay from 2.56 to 4 nm ($2\theta = 2.2^\circ$). Increasing the basal spacing of organoclay

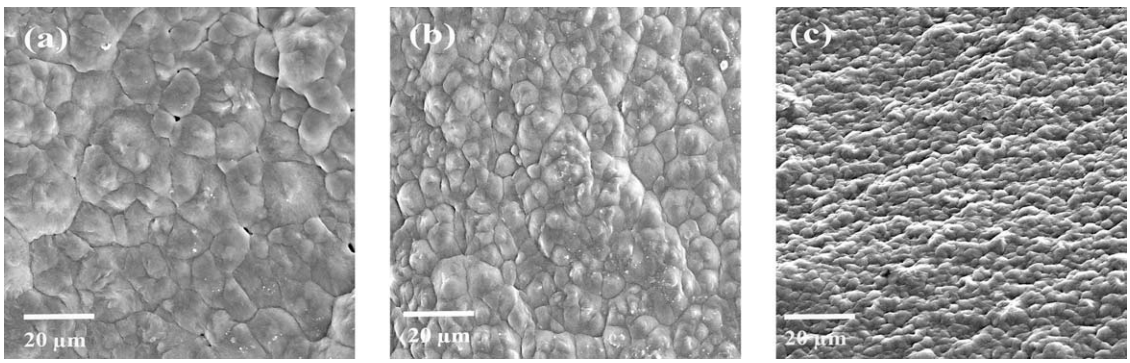

Figure 5 (a) Etched SEM photomicrograph of 50/50/0 sample; (b) etched SEM photomicrograph of 50/50/5-N sample; (c) etched SEM photomicrograph of 50/50/5 sample.

in the uncompatibilized nanocomposite samples when compared with pure cloisite 20A can be attributed to the proper modification of Na-MMT with dimethyl-dehydrogenated tallow that gives an intercalated morphology in the nanocomposites without grafting of MA.[29]

Scanning electron microscopy and TEM

Figure 5(a–c) shows the scanning electron microscopy (SEM) photomicrographs of cryogenically fractured of 50/50/0, 50/50/5-N, and 50/50/5 samples, respectively. It can be seen in Figure 5(a) that the rubber particles are dispersed throughout the LLDPE matrix in the form of aggregates also the size of rubber particles is about 14 μm in 50/50/0 sample. This behavior is attributed to the viscoelasticity of the rubber phase, as reported by Wu.[30] The etched fracture surface of 50/50/5-N sample is shown in Figure 5(b). It can be observed that the size of rubber particles slightly decreased to 8 μm by the introduction of the nanoclay. The change in the size of rubber particles of the TPV nanocomposites is explained by the modified rheology of the nanocomposites. It is well accepted that the size of the dispersed rubber phase in unfilled TPV materials (without nanoclay) depends on the viscosity ratio and interfacial interactions (tension) between two phases.[2] Therefore, the melt viscosity ratio of the reclaim dispersed phase to the LLDPE matrix (P = reclaim viscosity/LLDPE viscosity) is known to control the rubber particle coalescence and break-up process during shearing. In general, in the TPV nanocomposites, the organoclay particles play an important role to determine the morphology of the nanocomposites. Figure 5(c) shows the micrograph of the 50/50/5 sample (containing both nanoclay and compatibilizer). It can be seen that the agglomerate formation of rubber particles declined by the decreased rubber aggregate size resulting from the introduction of nanoclay and compatibilizer in the 50/50/5 sample.[31] Reclaimed rubber particles exhibit a reduction in the average size of particles as a result of nanoclay and compatibilizer loading. The effect of the nanoclay on the rheology of 50/50/5-N sample is shown in Figure 6. It can be seen that melt viscosity of 50/50/0 increased with the introduction of the nanoclay (50/50/5-N sample) at low frequency region. The change of the viscosity ratio between the two phases leads to decrease in the size of the rubber phase.

The effect of nanoclay on the rheology of samples is shown in Figure 6. The melt viscosity of 50/50/0 increased with the introduction of nanoclay (50/50/5-N sample). The change in the viscosity ratio between the two phases leads to a decrease in the size of the rubber phase. The melt viscosity of 50/50/0 sample strongly increased with the introduction of nanoclay and compatibilizer (50/50/5 sample). The change in the melt viscosity ratio due to addition of nanoclay and compatibilizer may be contributed to the reduction of size of dispersed particles.[32] Also, the reduction in the size of particles implies the reduction in the interfacial tension or better adhesion between LLDPE matrix and reclaimed rubber dispersed phase.[33] Incidentally, the

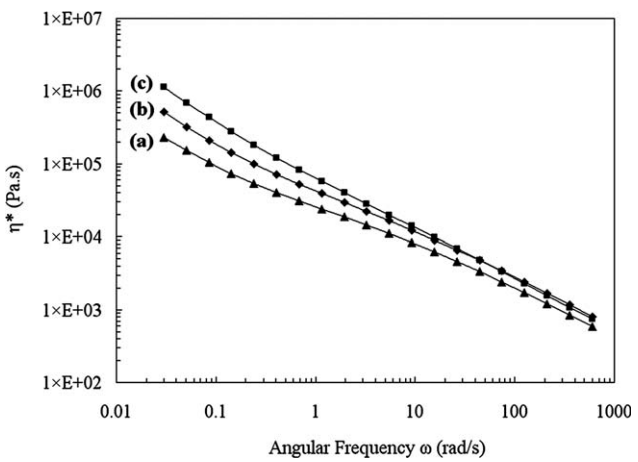

Figure 6 Complex viscosity as a function of frequency for (a) 50/50/0, (b) 50/50/5-N, and (c) 50/50/5.

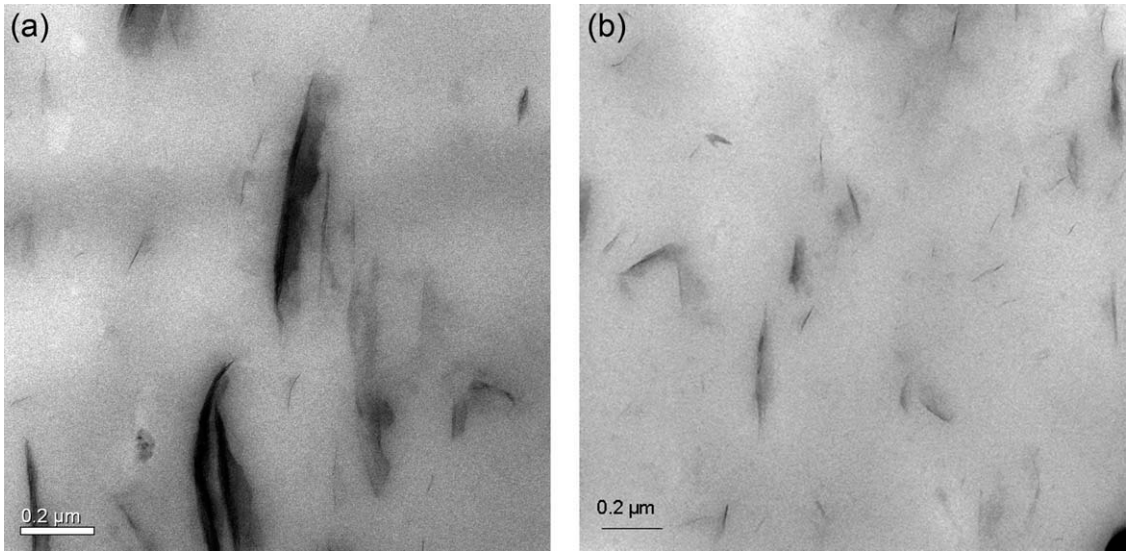

Figure 7 (a) TEM image of 50/50/5-N; (b) TEM image of 50/50/5.

nanoclay platelets and compatibilizer may act as interfacial agents, reducing the interfacial tension with a concomitant break up of the reclaim particles and a reduction in the size of particles in TPV nanocomposite based on 50 wt % reclaimed rubber and 5 wt % nanoclay.[32]

Figure 7(a) shows the TEM image of the nanocomposite prepared by using LLDPE and reclaimed rubber without compatibilizer. The LLDPE phase is white in color, and silicate layers appear as black lines in the darker reclaimed rubber phase. For the uncompatibilized nanocomposite (50/50/5-N) at 5 wt % of nanoclay, large aggregates of the nanoclay particles can exist as in conventional composites. For the nanocomposite prepared by LLDPE/reclaim containing 5 wt % of nanoclay, the number of clay aggregates is diminished by incorporating the compatibilizer as shown in Figure 7(b). These results are in accordance with the intensity of the XRD patterns observed for the nanocomposites.

Mechanical properties

Table IV presents the mechanical properties of the TPV nanocomposite samples. It is observed that the tensile modulus, tensile strength, and hardness of the TPV nanocomposites decrease when the rubber content of the TPV samples is increased. This is explained to be due to the decrease in the concentration of semicrystalline LLDPE as the continuous phase. In fact, the decrease in modulus and tensile strength of TPV samples is because of the lower modulus and tensile strength of reclaimed rubber than those of LLDPE matrix, and also it is because of the decrease in the concentration of semicrystalline LLDPE. Table IV also shows that the increase in

TABLE IV
Mechanical Properties of TPV Nanocomposites

Sample codes LL/Re/Clay	Tensile modulus (MPa)	Elongation at break (%)	Tensile strength (MPa)	Hardness (ShoreD)
90/10/0	111 ± 7.77	85 ± 5.1	13 ± 0.78	90 ± 3.6
90/10/3	127 ± 10.16	82 ± 6.56	11.5 ± 0.57	97 ± 2.91
90/10/5	136 ± 10.88	80.2 ± 5.6	11 ± 0.55	98 ± 4.9
90/10/7	138 ± 11.04	78 ± 4.68	10.6 ± 0.84	99 ± 4.95
70/30/0	67 ± 6.03	132 ± 11.88	8 ± 0.56	71 ± 4.26
70/30/3	75 ± 5.25	126 ± 10.08	7.5 ± 0.45	76 ± 3.8
70/30/5	87 ± 4.35	100 ± 6	6.9 ± 0.48	78 ± 3.12
70/30/7	90 ± 5.4	98 ± 5.88	6.5 ± 0.39	79 ± 4.74
50/50/0	43 ± 2.58	698 ± 55.84	5.6 ± 0.44	50.2 ± 3.51
50/50/3	53 ± 4.24	590 ± 53.1	5.6 ± 0.5	55.5 ± 3.88
50/50/5	55 ± 3.85	560 ± 39.2	5 ± 0.2	57 ± 3.42
50/50/7	57 ± 3.42	250 ± 17.5	5 ± 0.25	58 ± 1.74
50/50/3-N	29.64 ± 2.66	153 ± 12.24	5.19 ± 0.41	–
50/50/5-N	31.54 ± 1.89	148.9 ± 13	4.83 ± 0.28	–
50/50/7-N	32.89 ± 1.31	140 ± 8.4	4.63 ± 0.27	–

the rubber contents enhances elongation at break of samples. This is due to the higher elongation at break of rubber than that of thermoplastic matrix.

The mechanical properties of the compatibilized TPV nanocomposites prepared with 50 wt % RR and different nanoclay contents were compared to similar but uncompatibilized blends. It is seen that the mechanical properties are poor in uncompatibilized samples in comparison with compatibilized samples. It can be attributed to poor adhesion between interface of dispersed phase and LLDPE matrix that facilitates the propagation of cracks, and leads to a significant decline in the mechanical properties.

To improve the adhesion between interface of reclaimed rubber and polymer matrix, some interactions must be formed at the interface; therefore, MA-grafted polyethylene (PE-*g*-MA) is used as a reactive reagent to reduce the energy barrier and consequently, enhances interphase miscibility.[34] The improvement in the mechanical properties can be explained by the good adhesion between RR and LLDPE related to the addition of the compatibilizer PE-*g*-MA. It is also observed in Table IV that the modulus of compatibilized TPV nanocomposites based on 50 wt % RR is at range of 73–78% higher than similar but uncompatibilized samples. Moreover, the elongation at break of samples is at range of 78–285% higher than similar but uncompatibilized samples. Also, the tensile strength does not significantly change with the addition of compatibilizer and approximately remains constant. Generally, the elongation at break of thermoplastic elastomers increases if there is sufficient adhesion between the matrix and the rubber, hence efficient stress transfer from the matrix to the dispersed phase occurred, resulting in an increase of elongation at break, so mechanical properties of TPV nanocomposite are amplified by the compatibilizer.[32]

It can be seen that the modulus of the nanoclay-reinforced TPV samples is improved in all compositions compared to similar but unfilled blends. This was accepted that the exfoliated silicate layers are mainly a responsible factor for the improvement of stiffness in nanocomposite materials. The increasing of the TPV nanocomposites modulus is due to the presence of polar anhydride group, which enhances dipole and/or hydrogen bonding between the organoclay surface and the maleated polyethylene, causing to improve dispersion, intercalation, and adhesion of clay in polymer matrix.[35] Elongation at break of LLDPE/RR nanocomposites decreases with loading of the nanoclay. This behavior is explained by the formation of the strong interaction between nanoclay and polymer matrix, which reduces the molecular mobility of polymer chains.[36]

The tensile strength of the TPV nanocomposites slightly decreases with increasing nanofiller contents.

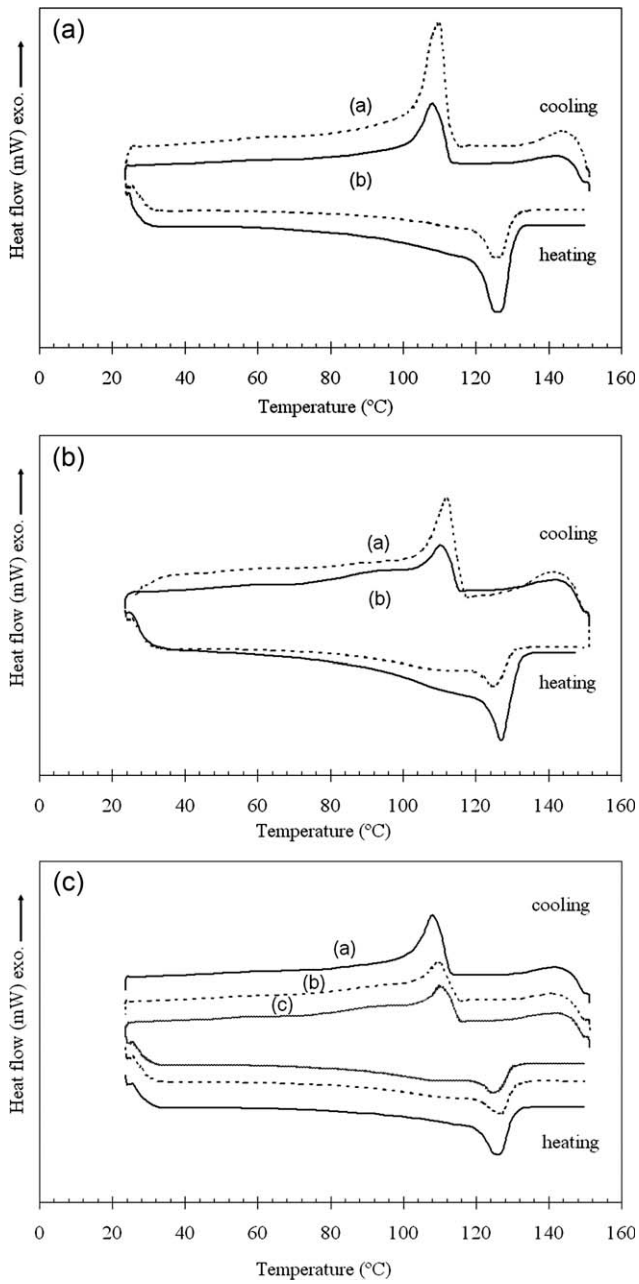

Figure 8 A: DSC thermograms of (a) 90/10/0 and (b) 50/50/0; B: DSC thermograms of (a) 90/10/7 and (b) 50/50/7; C: DSC thermograms of (a) 50/50/0, (b) 50/50/5, and (c) 50/50/7.

Many researches have shown that tensile strength is decreased with increasing nanoclay contents.[2,37,38] The improvement in the mechanical properties of a filled system depended on the filler type and extent is reported in many studies.[1,2,39]

Table IV shows the effect of nanoclay contents on the hardness of LLDPE/RR nanocomposites prepared with 10, 30, and 50 wt % RR. It can be seen that the loading of the nanoclay increases the hardness of TPV nanocomposite samples, whereas the increasing the reclaimed rubber content reduces the hardness. The

TABLE V
Thermal Properties of the Samples

Sample codes	T_C (°C)	ΔH_C (J/g)	T_m (°C)	ΔH_m (J/g)	T_C onset (°C)
90/10/0	109.4	85.56	126.1	98.53	119
90/10/7	112.1	82.97	127.4	76.51	118
50/50/0	108.4	47.94	125.7	52.95	117
50/50/5	109.9	42.86	126.4	43.3	117
50/50/7	110.6	39.16	126.5	39.59	115

reduction in hardness is due to the lower hardness of the RR than that of LLDPE. In the presence of the reinforcing nanoclay, the higher hardness degree is achieved due to the polymer–nanoclay interaction.[40]

Thermal and crystallization characteristics by differential scanning calorimetry

The thermal characteristics of TPV nanocomposites of LLDPE/RR were studied using DSC cycle of melting-crystallization-melting. The melting behavior of a polymer depends on several factors such as thermal history and the heating rate selected during the measurement. For the thermal studies, the present work focused on the effects of rubber and nanoclay contents on the thermal behavior of the TPV nanocomposites.

Figure 8(a,b) shows the DSC curves of cooling and heating scan for unfilled and filled TPV samples (7 wt % nanoclay) containing 10 and 50 wt % RR. As it can be seen in Figure 8(a,b), the crystallization temperature (T_C) and melting temperature (T_m) slightly decreased when the rubber content was increased from 10 to 50 wt % for unfilled and filled samples containing 7 wt % nanoclay (Table V provides more touchable data). The changes in T_m and T_C reflect the interference during the formation of the crystalline part of LLDPE. It would be attributed to the presence of reclaimed rubber that would interfere with the crystallization of polyethylene. It may mean that some crystalline regions of LLDPE are destroyed due to the interference in the form of reclaim molecular incorporation into the LLDPE part and T_m and T_C decreased with an increasing of reclaimed content.[9] It is well known that the decrease in T_m is caused by the formation of imperfect crystallites or by crystallites having smaller size.[41] Table V summarizes the thermal characteristics of various TPV nanocomposite samples. It can be seen that the melting enthalpy (ΔH_m) and crystallization enthalpy (ΔH_C) decreased with increasing rubber contents.

Figure 8(c) shows the DSC result of TPV nanocomposites (5 and 7 wt % nanoclay) and unfilled samples based on 50 wt % RR. Figure 8(c) indicates that the T_C and T_m slightly increased by increasing of nanoclay contents reflecting the effect that the filler has on the crystal nucleation. In the field of TPV nanocomposites, an increase in the T_C is generally expected to accrue, due to the promotion of a heterogeneous nucleation by the nanoparticles,[17] and formation of smaller crystals, which could result from a nucleation effect of nano particles. The increase in T_m could be resulted from the fact that the dispersed platelets in the matrix may shield the conduction of heat to crystallites to some extent until at higher temperatures that heat flow is enough to melt down the crystallites.[42] However, enthalpy of melting of polyethylene followed an opposite trend indicating decrease in crystallinity content is shown in Table V. It seems that exfoliated/intercalated organoclay platelets may reduce the growth of polyethylene spherulites and disrupt the crystallization process.[42]

CONCLUSIONS

In this work, we examined morphological, thermal, and mechanical properties of the nanoclay-reinforced dynamically vulcanized TPE nanocomposites based on LLDPE/reclaimed rubber containing 10, 30, and 50 wt % RR additionally 3, 5, and 7 wt % nanoclay. The compounding process itself was found to be instrumental in the final dispersion state of the silicate layers. The interlayer distance is first increased by the incorporation of the filler in the LLDPE to obtain LLDPE nanocomposites. In this stage, we used PE-*g*-MA that acts as a compatibilizer for the nonpoplar LLDPE. Finally, intercalation and partial exfoliation are achieved by the shear stress developed during process of the mixing with RR and the vulcanization of rubber phase that increase viscosity. X-ray results showed that intercalated structure in the TPV nanocomposites was developed. The degree of intercalation of the nanoclay improved with the introduction of PE-*g*-MA in the TPV nanocomposites and the silicate layer aggregates considerably decreased with increasing of the rubber content. The TEM images showed that the nanolayers of clay platelets are dispersed randomly in the polymer matrix in compatibilized TPV nanocomposite. This result is supported by XRD data.

The results of the SEM photomicrographs of etched sample showed that the size of rubber

particles was reduced with the introduction of the nanoclay particles and compatibilizer.

The intercalated structure results an increase in the crystallization temperature, because the dispersed silicates acted as nucleating agents and may lead to the formation of smaller crystals. The DSC results showed that the T_C and T_m slightly increased by nanoclay loading; however, ΔH_m decreased when nanoclay concentration increased in TPV nanocomposites.

Moreover, the modulus and hardness of the TPV nanocomposite samples increased in comparison with the pristine TPVs; however, the elongation at break and tensile strength values continuously decreased as clay concentration increased in samples.

References

1. Naderi, G.; Lafleur, P. G.; Dubois, C. Int Polym Proc 2007, 22, 284.
2. Naderi, G.; Lafleur, P. G.; Dubois, C. Polym Eng Sci 2007, 47, 207.
3. Katbab, A. A.; Nazockdast, H.; Bazgir, S. J Appl Polym Sci 2000, 75, 1127.
4. Garces, J. M.; Moll, D. J.; Bicerano, J.; Fibiger, R.; McLeod, D. G. Adv Mater 2000, 12, 1835.
5. Adhikari, B.; De, D.; Maiti, S. Prog Polym Sci 2000, 25, 909.
6. Farahani, T. D.; Bakhshandeh, G. R.; Abtahi, M. Polym Bull 2006, 56, 495.
7. Koning, C.; Van Duin, M.; Pagnoulie, C.; Jerome, R. Prog Polym Sci 1998, 23, 707.
8. Ahmad, A.; Dahlan, H. M.; Abdullah, I. Iranian Polym J 2003, 12, 381.
9. Magaraphan, R.; Skularriya, R.; Kohjiya, S. J Appl Polym Sci 2007, 105, 1914.
10. Abadchi, M. R.; Arani, A. J.; Nazockdast, H. J Appl Polym Sci 2010, 115, 2416.
11. Punnarak, P.; Tantayanon, S.; Tangpasuthadol, V. Polym Degrad Stab 2006, 91, 3456.
12. Kumar, C. R.; Fuhrmann, I.; Karger-Kocsis, J. Polym Degrad Stab 2002, 76, 137.
13. Scaffaro, R.; Dintcheva, N. T.; Nocilla, M. A.; La mantia, F. P. Polym Degrad Stab 2005, 90, 281.
14. Aso, O.; Eguiazabal, J. I.; Nazabal, J. Compos Sci Technol 2007, 67, 2854.
15. Sheng, N.; Boyce, M. C.; Parks, D. M.; Rutledge, G. C.; Abes, J. I.; Cohen, R. E. Polymer 2004, 45, 487.
16. Hotta, S.; Paul, D. R. Polymer 2004, 45, 7639.
17. Truss, R. W.; Yeow, T. K. J Appl Polym Sci 2006, 100, 3044.
18. Durmus, A.; Woo, M.; Kasgoz, A.; Macosko, C. W.; Tsapatsis, M. Eur Polym J 2007, 43, 3737.
19. Stoeffler, K.; Lafleur, P. G.; Denault, J. Polym Eng Sci 2008, 48, 1449.
20. Jin, D. W.; Seol, S. M.; Kim, G. H. J Appl Polym Sci 2009, 114, 25.
21. Guo, C. Y.; Ke, Y.; Liu, Y.; Mi, X.; Zhang, M.; Hu, Y. Polym Int 2009, 58, 1319.
22. Varghese, S.; Karger-Kocsis, J.; Catos, K. G. Polymer 2003, 44, 3977.
23. Sun, Y.; Luo, Y.; Jia, D. J Appl Polym Sci 2008, 107, 2786.
24. Li, P.; Wang, L.; Song, G.; Yin, L.; Qi, F.; Sun, L. J Appl Polym Sci 2008, 109, 3831.
25. Naderi, G.; Lafleur, P. G.; Dubois, C. Polym Compos 2008, 29, 1301.
26. Durmus, A.; Kasgoz, A.; Macosko, C.W. Polymer 2007, 48, 4492.
27. Lew, C. Y.; Murphy, W. R.; McNally, G. M. Polym Eng Sci 2004, 44, 1027.
28. Kato, M.; Usuki, A.; Okada, A. J Appl Polym Sci 1997, 66, 1781.
29. Wang, K. H.; Choi, M. H.; Koo, C. M.; Choi, Y. S.; Chung, I. J. Polymer 2001, 42, 9819.
30. Wu, S. Polym Eng Sci 1987, 27, 335.
31. Wang, Z.; Qu, B.; Fan, W.; Hu, Y., Shen, X. Polym Degrad Stab 2002, 76, 123.
32. Phinyocheep, P.; Axtell, F. H.; Laosee, T. J Appl Polym Sci 2002, 86, 148.
33. Towichayathamrong, C.; Mojdara, B.; Jamieson, A. M.; Martin, D. C. JI metals mater miner 2001, 10, 52.
34. Li, Y.; Zhang, Y.; Zhang, Y. J Appl Polym Sci 2003, 88, 2020.
35. Mehrabzadeh, M.; Kamal, M. R.; Quintanar, G. Iranian Polym J 2009, 18, 833.
36. Supri, A. G.; Salmah, H.; Hazwan, K. Malay Polym J 2008, 3, 39.
37. Naderi, G.; Razavi-Nouri, M.; Taghizadeh, E.; Lafleur, P. G.; Dubois, C. Polym Eng Sci 2011, 51, 278.
38. Mahallati, P.; Arefazar, A., Naderi, G. Int Polym Process 2010, 2, 132.
39. K.Mishra, J.; Kim, G. H.; Kim, I. I.; Chung, I. J.; Ha, C. S. J Polym Sci Part B: Polym Phys 2004, 42, 2900.
40. Mandal, U. K.; Aggarwal, S. Polym Test 2001, 20, 305.
41. Qin, J.; Ding, H.; Wang, X.; Xie, M.; Yu, Z. Polym-Plast Technol Eng 2008, 47, 199.
42. Dadbin, S.; Noferesti, M.; Frounchi, M. Macromol Symp 2008, 274, 22.